FINITE DIFFERENCE SOLUTION OF UNSTEADY FREE CONVECTION HEAT AND MASS TRANSFER FLOW PAST A VERTICAL PLATE

Md. Arifuzzaman[1], Rabindra Nath Mondal[2]

[1] Department of General Educational Development, Faculty of Science and Information Technology
Daffodil International University, Dhanmondi, Dhaka, Bangladesh
[2] Department of Mathematics, Jagannath University, Dhaka-1100, Bangladesh

Email: rfzmn.du@gmail.com

Abstract: *An analysis is performed numerically to study the unsteady free convection heat and mass transfer flow past a semi-infinite vertical flat plate by using finite difference method. First, thermal boundary layer equations have been derived from the Navier-Stokes equation and concentration equation by boundary layer technique. Second, some non-dimensional variable has been introduced to make these equations dimensionless. Then Finite difference method is used to solve these equations. The solution of heat and mass transfer flow is studied examining the velocity, temperature and concentration distribution. The effects on the velocity profiles, temperature profiles and concentration profiles for various parameters have been separately discussed and shown graphically.*

Keywords: *Thermal boundary layer, heat transfer, finite difference, velocity profile.*

1. Introduction

Investigation of thermal boundary layer flow of an electrically conducting fluid past a vertical heated surface has attracted the interest of many researchers because of its important applications in many engineering problems such as in plasma studies, petroleum industries, power generators, cooling of nuclear reactors, the boundary layer control in aerodynamics, and crystal growth. The boundary layer equation has the capacity to admit a large number of invariant closed-form solutions. On the other hand, the problem of mixed convection due to a heated or cooled vertical flat plate provides one of the most basic scenarios for heat transfer theory and thus is of considerable theoretical and practical interest which has been extensively studies by Sparrow et al. [1], Banthiya [2], Hussain and Afzal [3], Merkin [4] and Watanabe [5].

In light of the work of Cess [6], Mansour [7] studied the interaction of mixed convection with thermal radiation in laminar boundary layer flow over a horizontal, continuous moving sheet with suction and injection. Bestman [8] made a study of a laminar natural convection boundary layer in porous medium making a very simple model of a binary reaction with Arrhenius activation energy. Afterwards a mathematical approach to this problem in case of a steady flow was made by Alabraba et. al.[9]. They considered the problem of free convection interaction with thermal radiation in a hydromagnetic boundary layer taking into account the chemical reaction. Das et al. [10] investigated the effects of mass transfer on flow past an impulsively started infinite vertical plate with constant heat flux in the presence of chemical reaction.

Finite difference method is used mostly in numerical analysis, especially in numerical differential equations, main purpose for the numerical solution of ordinary, partial differential and thermal boundary layer equations respectively. The main idea, replacing the derivatives appearing in the differential equation by finite differences that approximate them. Finite difference methods are used in science and engineering disciplines such as thermal engineering, fluid mechanics, etc. Sattar and Alam [11] employed explicit finite difference method to study unsteady free convection and mass transfer flow of a viscous,

Incompressible and electrically conduction fluid past a moving infinite vertical porous plate with thermal diffusion effect. Alam et al. [12] performed finite difference solution of heat and

Date of submission : 30.01.2017 Date of acceptance : 04.04.2017

mass transfer flow in vertical porous plate with induced magnetic field.

The solution, made by Finite difference method is one of the most interesting choices to the researcher. Alam and Sattar [13] investigated heat transfer in thermal boundary layers of magneto-hydrodynamic flow over a flat plate. Alam et al. [14] studied combined free and forced convection mass transfer flow past a vertical porous plate with heat generation and thermal diffusion. Recently, Islam et al. [15] investigated unsteady solutions of thermal boundary layer equations for heat and mass transfer flow by using finite difference method, and examined the velocity, temperature and concentration distribution characteristics. To study the heat transfer characteristics in boundary layer flow of a Newtonian fluid, Chamkha and Khaled [16] investigated the problem of coupled heat and mass transfer by hydro-magnetic free convection from an inclined plate in the presence of internal heat generation or absorption, and similarity solutions were presented. Reddy and Reddy [17] performed an analysis to study the natural convection flow over a permeable inclined surface with variable temperature, momentum and concentration. Recently, Hasanuzzaman et al. [18] studied the similarity solution of unsteady combined free and force convective laminar boundary layer flow about a vertical porous surface with suction and blowing.

In the present study, finite difference scheme is used to find out the solution of heat and mass transfer flow past a vertical plate, and examine the velocity, temperature and concentration distribution characteristics. Three kind of profiles as velocity, temperature and concentration profiles are separately discussed with graphics.

2. Mathematical model and governing equations of the flow

Consider an unsteady laminar, incompressible, viscous fluid streaming through a semi-infinite vertical flat plate. Initially, the density and temperature of the fluid and the flow velocity pattern are assumed to be uniform which is similar to that of the fluid outside the boundary layer. The flow is chosen along the plate in the x- direction and y axis is taken to be normal to it in the Cartesian coordinate system. Initially we consider that everywhere in the fluid (plate), the temperature $T(T_\infty)$ level and the concentration level $C(C_\infty)$ are same. Also assumed that the fluid and the plate are at rest. After that the plate is to be moving with a constant velocity U_0 in its own plane and instantaneously at time t > 0, the concentration and the temperature of the plate are raised to $C_w(>C_\infty)$ and $T_w(>T_\infty)$ respectively, which are thereafter maintained constant, where C_w, T_w are species concentration and temperature at the wall of the plate and C_∞, T_∞ are the concentration and temperature of the species far away from the plate respectively. The flow configuration & the Cartesian coordinate system of the study are shown in Figure 1.

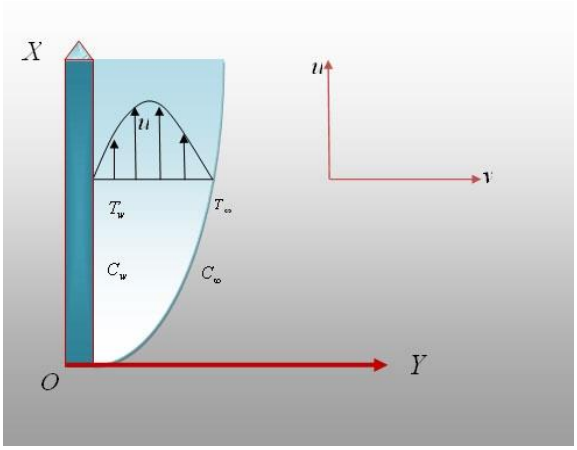

Figure 1: Flow configuration and Cartesian coordinate system

Within the framework of the above stated assumptions with reference to the generalized equations described before the equation relevant to the transient two dimensional problems are governed by the following system of coupled non-linear differential equations.

Equation of Continuity:

$$\frac{\partial u}{\partial x}+\frac{\partial v}{\partial y}=0 \qquad (1)$$

Equation of Momentum:

$$\frac{\partial u}{\partial t}+u\frac{\partial u}{\partial x}+v\frac{\partial v}{\partial y}=v\frac{\partial^2 u}{\partial y^2}+g\beta(T-T_\infty)+g\beta^*(C-C_\infty) \qquad (2)$$

Equation of Energy:

$$\frac{\partial T}{\partial t}+u\frac{\partial T}{\partial x}+v\frac{\partial T}{\partial y}=\frac{K}{\rho C_p}\frac{\partial^2 T}{\partial y^2}+Q\left(T_\infty-T\right) \qquad (3)$$

Equation of Concentration:

$$\frac{\partial C}{\partial t}+u\frac{\partial C}{\partial x}+v\frac{\partial C}{\partial y}=D\frac{\partial^2 C}{\partial y^2} \qquad (4)$$

With the corresponding initial and boundary conditions:

At $t=0 \quad u=0, v=0, T\to T_\infty, C\to C_\infty$

everywhere (5)

$$t>0\begin{cases}u=0,\ v=0,\ T\to T_\infty,\ C\to C_\infty \ \ at\ x=0\\ u=0,\ v=0,\ T\to T_w,\ C\to C_w \ at\ y=0\\ u=0,\ v=0,\ T\to T_w,\ C\to C_w \ as\ y\to\infty\end{cases} \qquad (6)$$

Where x, y are the Cartesian coordinate system, u, v are the velocity components along the *x* and *y* directions respectively. υ is the kinematic viscosity, *g* is the local acceleration due to gravity, C_p is the specific heat at the constant pressure ρ is the density of the fluid, K is the thermal conductivity, and D is the coefficient of mass diffusivity.

3. Mathematical Analysis

Since the solutions of the governing equations (1)-(4) under the initial condition (5) and boundary conditions (6) will be based on a finite difference method, it is required to make the said equations dimensionless. In order to obtain similarity solution, we introduce the following dimensionless variables:

$$X=\frac{xU_0}{\upsilon},\ Y=\frac{yU_0}{\upsilon},\ U=\frac{u}{U_0},\ V=\frac{v}{U_0},$$

$$\tau=\frac{tU_0^2}{\upsilon},\bar{T}=\frac{T-T_\infty}{T_w-T_\infty}\ and\ \bar{C}=\frac{C-C_\infty}{C_w-C_\infty}$$

Using these relations we have the following derivatives:

$$\frac{\partial u}{\partial t}=\frac{U_0^{\,3}}{\upsilon}\frac{\partial U}{\partial \tau},\frac{\partial u}{\partial x}=\frac{U_0^{\,2}}{\upsilon}\frac{\partial U}{\partial X},\frac{\partial u}{\partial y}=\frac{U_0^{\,2}}{\upsilon}\frac{\partial U}{\partial Y},$$

$$\frac{\partial u}{\partial y}=\frac{U_0^{\,2}}{\upsilon}\frac{\partial U}{\partial Y},\frac{\partial^2 u}{\partial y^2}=\frac{U_0^3}{\upsilon^2}\frac{\partial^2 U}{\partial Y^2},\frac{\partial v}{\partial y}=\frac{U_0^2}{\upsilon}\frac{\partial V}{\partial Y},$$

$$\frac{\partial T}{\partial x}=\frac{U_0\left(T_w-T_\infty\right)}{\upsilon}\frac{\partial \bar{T}}{\partial X};\ \frac{\partial T}{\partial y}=\frac{U_0\left(T_w-T_\infty\right)}{\upsilon}\frac{\partial \bar{T}}{\partial Y};$$

$$\frac{\partial^2 T}{\partial y^2}=\frac{U_0^{\,2}}{\upsilon^2}\left(T_w-T_\infty\right)\frac{\partial^2 \bar{T}}{\partial Y^2};\frac{\partial C}{\partial t}=\frac{U_0^{\,2}}{\upsilon}\left(C_w-C_\infty\right)\frac{\partial \bar{C}}{\partial \tau};$$

$$\frac{\partial C}{\partial x}=\frac{U_0}{\upsilon}\left(C_w-C_\infty\right)\frac{\partial \bar{C}}{\partial X};\frac{\partial C}{\partial y}=\frac{U_0}{\upsilon}\left(C_w-C_\infty\right)\frac{\partial \bar{C}}{\partial Y};$$

$$\frac{\partial^2 C}{\partial y^2}=\frac{U_0^{\,2}}{\upsilon^2}\left(C_w-C_\infty\right)\frac{\partial^2 \bar{C}}{\partial Y^2}$$

Now we substitute the values of the above derivatives into the equations (1)-(4) and by simplifying we obtain the following nonlinear coupled partial differential equations in terms of dimensionless variables.

$$\frac{\partial U}{\partial X}+\frac{\partial V}{\partial Y}=0 \qquad (7)$$

$$\frac{\partial U}{\partial \tau}+U\frac{\partial U}{\partial X}+V\frac{\partial U}{\partial Y}=\frac{\partial^2 U}{\partial Y^2}+G_r\bar{T}+G_m\bar{C} \qquad (8)$$

$$\frac{\partial \bar{T}}{\partial \tau}+U\frac{\partial \bar{T}}{\partial X}+V\frac{\partial \bar{T}}{\partial Y}=\frac{1}{Pr}\frac{\partial^2 \bar{T}}{\partial Y^2}-\alpha\bar{T} \qquad (9)$$

$$\frac{\partial \bar{C}}{\partial \tau}+U\frac{\partial \bar{C}}{\partial X}+V\frac{\partial \bar{C}}{\partial Y}=\frac{1}{S_c}\frac{\partial^2 \bar{C}}{\partial Y^2} \qquad (10)$$

where, $Gr=\frac{\upsilon g\beta\left(T_w-T_\infty\right)}{U_0^{\,3}}$ is the Grashof number, $Gm=\frac{\upsilon g^*\beta\left(C_w-C_\infty\right)}{U_0^{\,3}}$ is the modified Grashof number, $Pr=\frac{\upsilon\rho C_p}{K}$ is the Prandlt number, $S_c=\frac{\upsilon}{D}$ is the Schmidt number and $\alpha=\frac{Q\upsilon}{U_0^2}$ is the heat source parameter. The initial and boundary conditions are:

At $\tau=0 \quad U=0,\ V=0,\ \bar{T}=0,\ \bar{C}=0$

everywhere (11)

$$\tau > 0 \begin{cases} U = 0,\ V = 0, \bar{T} = 0, \bar{C} = 0 \ at\ X = 0 \\ U = 0,\ V = 0, \bar{T} = 1, \bar{C} = 1 \ at\ Y = 0 \\ U = 0,\ V = 0, \bar{T} = 0, \bar{C} = 0 \ as\ Y \to \infty \end{cases} \quad (12)$$

4. Numerical Computations

In this section, we attempt to solve the governing second order nonlinear coupled dimensionless partial differential equations with the associated initial and boundary conditions. Finite difference method has been used to solve the equations (7) - (10) subject to the initial conditions given by (11) and boundary conditions given by (12).

The region of the flow is divided into grid of lines to get the difference equation. The lines are parallel to X and Y axes (X -axes is taken along the plate and Y - axes is normal to the plate). We consider the plate of height $X_{\max}(=200)$ and regard $Y_{\max}(=20)$ as corresponding to $Y \to \infty$. Again, we consider the plate of height $X_{\max}(=100)$ and regard $Y_{\max}(=20)$ for *Pr* = 0.71 as corresponding to $Y \to \infty$. For *Pr* = 1.0 and *Pr* = 7.0 we have $m = 400, n = 400$ in X and Y axis grid spaces. Finally we will consider $m = 200$ and $n = 200$ in X and Y axis grid spaces for *Pr* = 0.71 which is shown in Fig. 2.

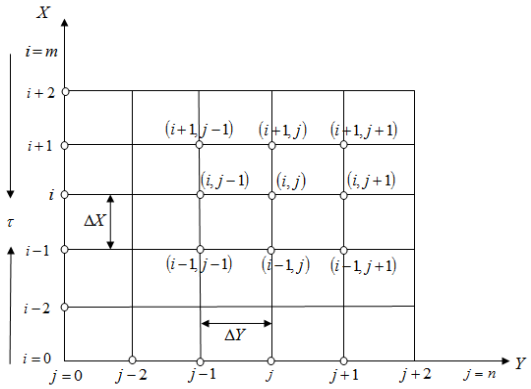

Figure 2: X and Y axis space grid

It is assumed that $\Delta X, \Delta Y$ are the constant mesh sizes along the X and Y directions respectively, and are taken as $\Delta X = 0.5\ (0 \le x \le 200)$ and $\Delta Y = 0.05\ (0 \le y \le 20)$. However, in the case of $Pr = 0.71$, ΔX and ΔY are taken as $\Delta X = 0.5\ (0 \le x \le 100)$ and $\Delta Y = 0.1\ (0 \le y \le 20)$ with the smaller time step $\Delta\tau = 0.001$. Now using the finite difference formula as below

$$\left(\frac{\partial U}{\partial \tau}\right)_{i,j} = \frac{U'_{i,j} - U_{i,j}}{\Delta\tau}, \left(\frac{\partial U}{\partial X}\right)_{i,j} = \frac{U_{i,j} - U_{i-1,j}}{\Delta X} \quad (13)$$

$$\left(\frac{\partial U}{\partial Y}\right)_{i,j} = \frac{U_{i,j+1} - U_{i,j}}{\Delta Y}, \left(\frac{\partial V}{\partial Y}\right)_{i,j} = \frac{V_{i,j} - V_{i,j-1}}{\Delta Y},$$

$$\left(\frac{\partial \bar{T}}{\partial \tau}\right)_{i,j} = \frac{\bar{T}'_{i,j} - \bar{T}_{i,j}}{\Delta\tau}; \left(\frac{\partial \bar{T}}{\partial X}\right)_{i,j} = \frac{\bar{T}_{i,j} - \bar{T}_{i-1,j}}{\Delta X};$$

$$\left(\frac{\partial \bar{T}}{\partial Y}\right)_{i,j} = \frac{\bar{T}_{i,j+1} - \bar{T}_{i,j}}{\Delta Y}, \left(\frac{\partial \bar{C}}{\partial \tau}\right)_{i,j} = \frac{\bar{C}'_{i,j} - \bar{C}_{i,j}}{\Delta\tau};$$

$$\left(\frac{\partial \bar{C}}{\partial X}\right)_{i,j} = \frac{\bar{C}_{i,j} - \bar{C}_{i-1,j}}{\Delta X}; \left(\frac{\partial \bar{C}}{\partial Y}\right)_{i,j} = \frac{\bar{C}_{i,j+1} - \bar{C}_{i,j}}{\Delta Y},$$

$$\left(\frac{\partial^2 U}{\partial Y^2}\right)_{i,j} = \frac{U_{i,j+1} - 2U_{i,j} + U_{i,j-1}}{(\Delta Y)^2};$$

$$\left(\frac{\partial^2 \bar{T}}{\partial Y^2}\right)_{i,j} = \frac{\bar{T}_{i,j+1} - 2\bar{T}_{i,j} + \bar{T}_{i,j-1}}{(\Delta Y)^2},$$

$$\left(\frac{\partial^2 \bar{C}}{\partial Y^2}\right)_{i,j} = \frac{\bar{C}_{i,j+1} - 2\bar{C}_{i,j} + \bar{C}_{i,j-1}}{(\Delta Y)^2} \quad (14)$$

Substituting the above relations into the corresponding differential equations we obtain an appropriate set of finite difference equations as follows,

$$V_{i,j} = V_{i,j-1} + \frac{U_{i-1,j} - U_{i,j}}{\Delta X}\Delta Y \quad (15)$$

$$U'_{i,j} = [\frac{U_{i,j+1} - 2U_{i,j} + U_{i,j-1}}{(\Delta Y)^2} + Gr\bar{T}_{i,j} + Gm\bar{C}_{i,j}$$
$$-U_{i,j}\frac{U_{i,j} - U_{i-1,j}}{\Delta X} - V_{i,j}\frac{U_{i,j+1} - U_{i,j}}{\Delta Y}]\Delta\tau + U_{i,j} \quad (16)$$

$$\frac{\bar{T}'_{i,j} - \bar{T}_{i,j}}{\Delta\tau} + U_{i,j}\frac{\bar{T}_{i,j} - \bar{T}_{i-1,j}}{\Delta X} + V_{i,j}\frac{\bar{T}_{i,j+1} - \bar{T}_{i,j}}{\Delta Y}$$
$$= \frac{1}{Pr}\frac{\bar{T}_{i,j+1} - 2\bar{T}_{i,j} + \bar{T}_{i,j-1}}{(\Delta Y)^2} - \alpha\bar{T}_{i,j} \quad (17)$$

$$\bar{C}'_{i,j} = [\frac{1}{Sc}\frac{\bar{C}_{i,j+1} - 2\bar{C}_{i,j} + \bar{C}_{i,j-1}}{(\Delta Y)^2} - U_{i,j}\frac{\bar{C}_{i,j} - \bar{C}_{i-1,j}}{\Delta X}$$
$$-V_{i,j}\frac{\bar{C}_{i,j+1} - \bar{C}_{i,j}}{\Delta Y}]\Delta\tau + \bar{C}_{i,j} \quad (18)$$

The initial and boundary conditions with the finite difference scheme are

$$U_{i,j}^{0}=0,\ V_{i,j}^{0}=0,\ \bar{T}_{i,j}^{0}=0,\bar{C}_{i,j}^{0}=0 \qquad (19)$$

$$\left.\begin{aligned} U_{0.j}^{n}&=0,\ V_{0,j}^{n}=0,\ \bar{T}_{0,j}^{n}=0,\bar{C}_{0,j}^{n}=0\\ U_{i,0}^{n}&=0,\ V_{i,0}^{n}=0,\ \bar{T}_{i,0}^{n}=1,\ \bar{C}_{i,0}^{n}=1\\ U_{i,L}^{n}&=0,\ V_{i,L}^{n}=0,\ \bar{T}_{i,L}^{n}=0,\ \bar{C}_{i,L}^{n}=0 \end{aligned}\right\} \qquad (20)$$

Here the subscripts i and j designate the grid points with *x*- and *y*-coordinates respectively, and the superscript n represents a value of time, $\tau=n\Delta\tau$, where $n=0,1,2,3.....$. During any one time step, the coefficients $U_{i,j}$ and $V_{i,j}$ appearing in equations (13)-(14) are created as constants.

Then at the end of any time-step $\Delta\tau$, the temperature $\overline{T}'$, the concentration $\overline{C}'$, the new velocity U', the new induced field V' at all interior nodal points may be obtained by successive applications of equations (15) - (18) respectively. This process is repeated in time and provided that the time-step is sufficiently small, U, V, $\overline{T}$, $\overline{C}$ should eventually converge to values which approximate the steady-state solution of equations (15)-(18). The steady- state or converged solutions of these equations are shown graphically in nine different figures.

5. Results and Discussions

The main goal of the computation is to obtain the steady-state solutions for the non-dimensional velocity U, temperature $\overline{T}$ and concentration $\bar{C}$ for different values of Prandtl number (Pr), the Grashof number (Gr), the modified Grashof number (Gm), the Schmidt number (Sc) and the heat source parameter (α). For this purpose, computations have been carried out up to dimensionless time τ = 80. The results of the calculations show graphical changes when time τ = 40 and at $\tau=(50-80)$ graphical change are negligible. Therefore the solution for dimensionless time τ =80 is necessarily steady-state solutions.

The solutions for the transient values of U versus Y, $\overline{T}$ versus Y, $\overline{C}$ versus Y along with the steady state solutions are displayed for different values of the parameters. In this paper, three values of the Prandtl numbers are considered. They are *Pr* = 7.00 (water), *Pr = 0.71* (air at 20^0), *Pr = 1.00* (salt water). Three values of *Sc*, *Gr*, *Gm* and α are however chosen randomly. From Figure 3(a), we see that the velocity profile increases as Grashof number increases at time $\tau=10$ and the velocity profile remains unchanged with the increasing of time which is shown in Figure 3(b), Figure 3(c) and Figure 3(d).

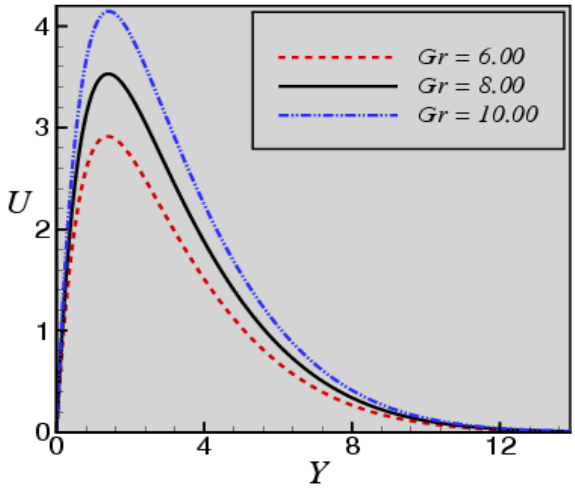

(a)

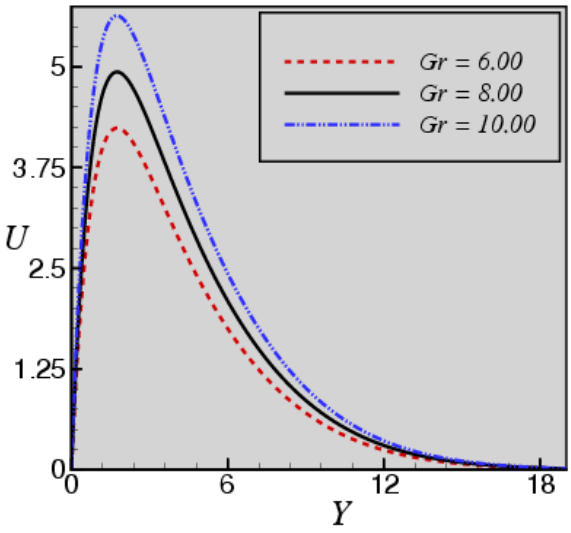

(b)

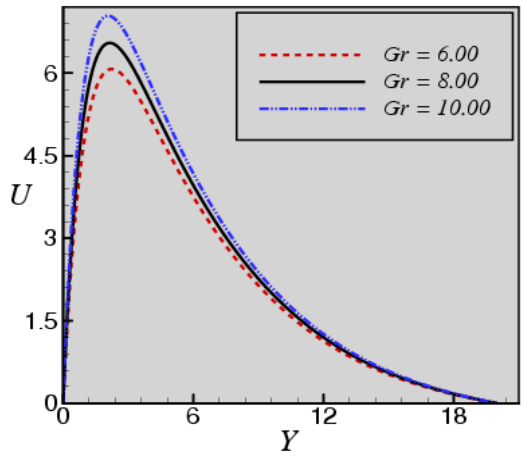

(c)

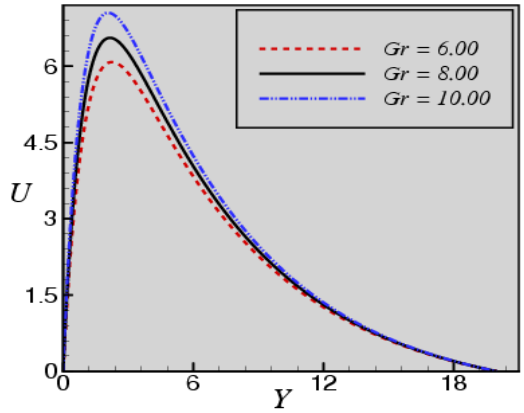

(d)

Figure 3: Velocity profile for Gr at $Pr = 1.0$, $\alpha = 2.0$, $Gm = 3.0$, $Sc = 15.0$, (a) $\tau = 10$, (b) $\tau = 20$, (c) $\tau = 50$ and (d) $\tau = 80$

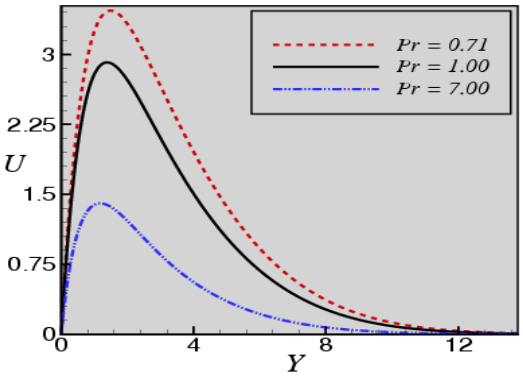

(a)

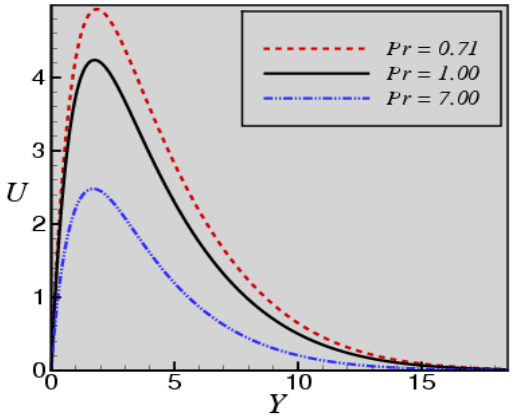

(b)

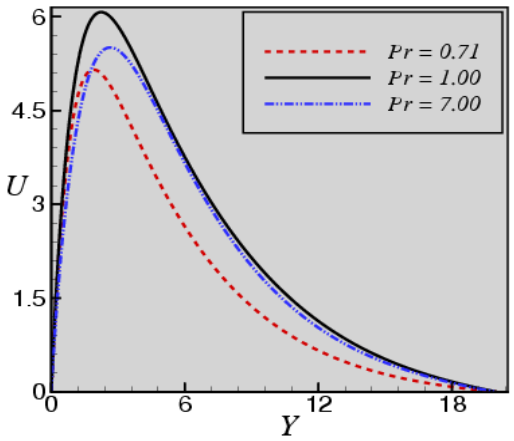

(c)

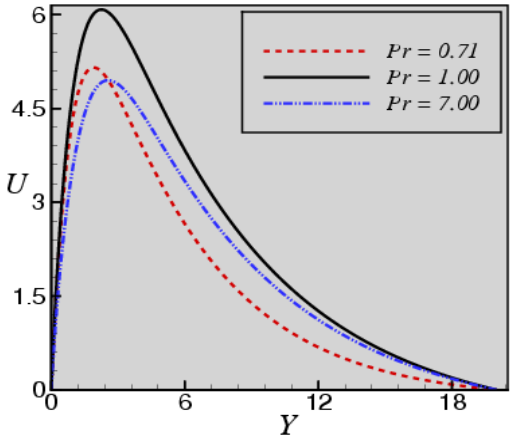

(d)

Figure 4: Velocity profile for Pr at $\alpha = 2.00$, $Gr = 6.00$, $Gm = 3.00$, $Sc = 15.00$ (a) $\tau = 10$, (b) $\tau = 20$, (c) $\tau = 50$ and (d) $\tau = 80$.

Figures 4(a) and 4(b) show that the velocity profile decreases with the increase of *Pr* at time $\tau = 10, 20$ but at time $\tau = 50,\ 80$ the velocity profile increases at *Pr* = 0.71, 1.0, which is shown in Figure 4(c) and Figure 4(d). We also observe that at *Pr* = 7.00 at time $\tau = 50,\ 80$ the velocity profile decreases. Figure 5 shows the effects of temperature distribution at various values of *Pr* with respect to time. We also observe that at different time if the values of *Pr* increases then the temperature profile decreases accordingly. Finally we see that at *Pr* = 7.0 the rate of change of temperature is low.

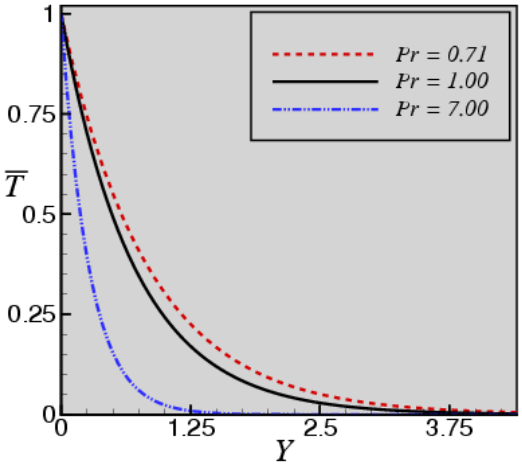

(a)

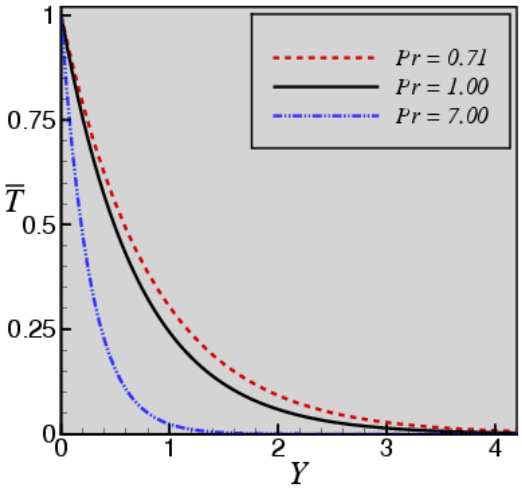

(b)

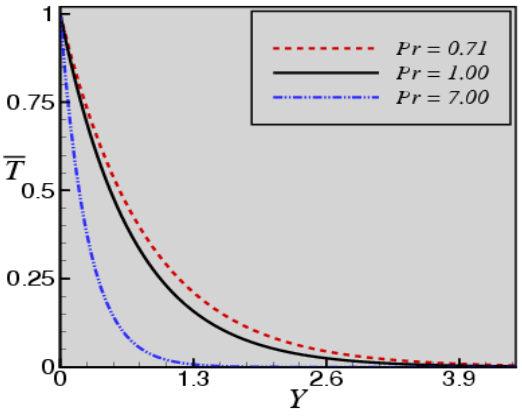

(c)

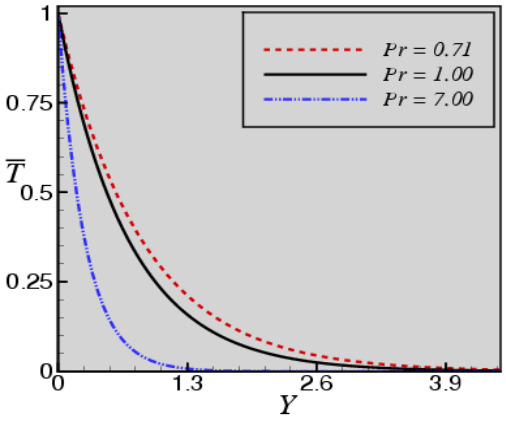

(d)

Figure 5: Temperature profile for *Pr* at $\alpha = 2.00$, $Gr = 6.00$, $Gm = 3.00$, $Sc = 15.00$ (a) $\tau = 10$, (b) $\tau = 20$, (c) $\tau = 50$ and (d) $\tau = 80$.

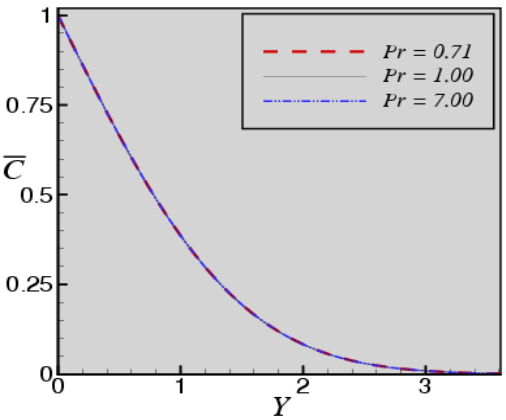

(a)

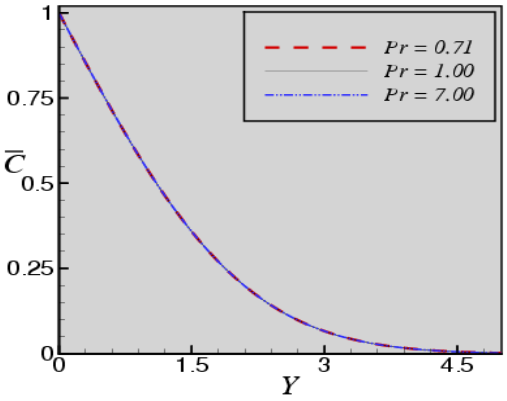

(b)

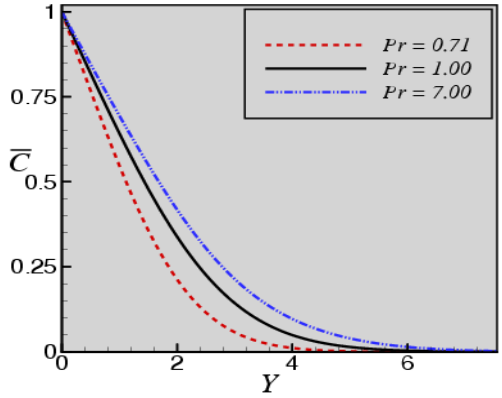

(c)

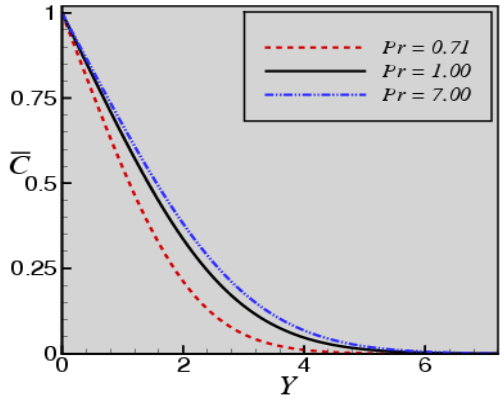

(d)

Figure 6: Concentration profile for Pr at $\alpha = 2.00$, $Gr = 6.00$, $Gm = 3.00$, $Sc = 15.00$ (a) $\tau = 10$ (b) $\tau = 20$ (c) $\tau = 50$ (d) $\tau = 80$.

Figure 6 shows the concentration profile for different values of *Pr* and from Figure 6(a) and Figure 6(b), we found that the concentration profile is steady at time $\tau = 10, 20$ but Figure 6(c) and Figure 6(d) show that the concentration profile increases with the increases of *Pr* at time $\tau = 50, 80$. Figure 7 represents the velocity profile for different values of *Gm* number at different times. From Figure 7 we observed that with the increase of *Gm*, velocity profile increases at different times. Figure 8 represents the concentration profile for different values of the Schmidt number at different time. We observe that concentration profile decreases with the increase of *Sc* at different time.

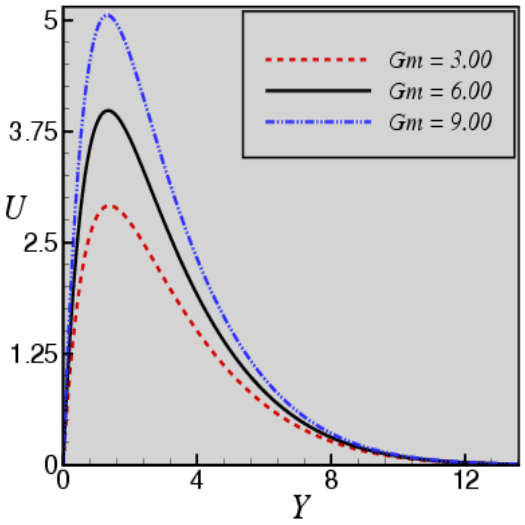

(a)

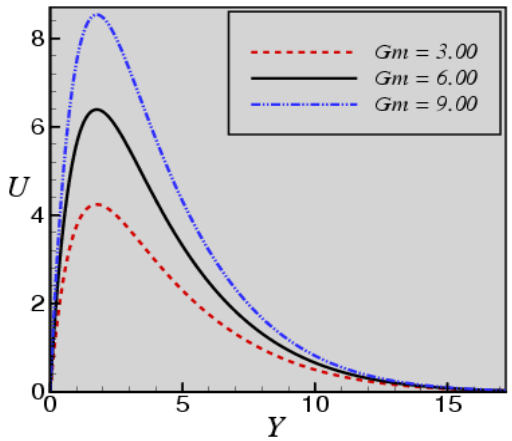

(b)

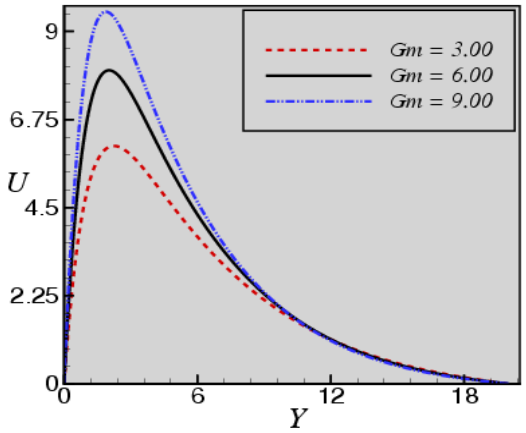

(c)

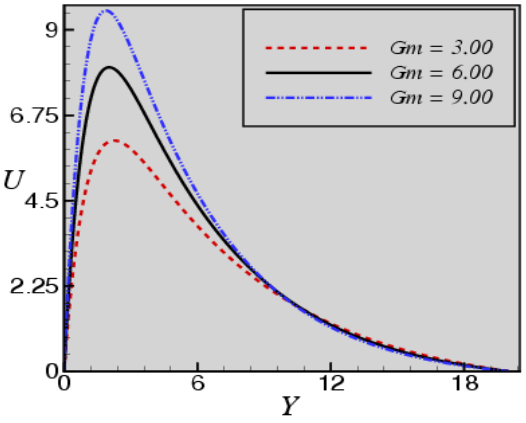

(d)

Figure 7: Velocity profile for Gm at $Pr = 1.00$, $\alpha = 2.00$, $Gr = 6.00$, $Sc = 15.00$ (a) $\tau = 10$ (b) $\tau = 20$ (c) $\tau = 50$ (d) $\tau = 80$

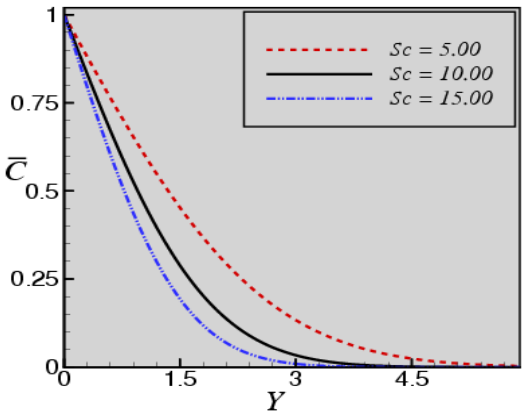

(a)

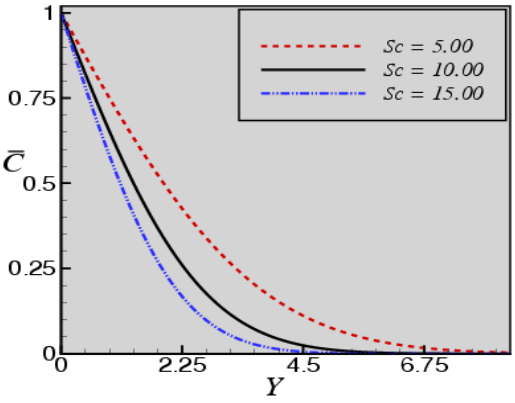

(b)

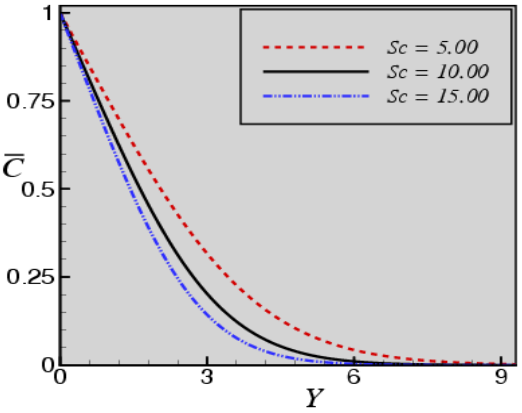

(c)

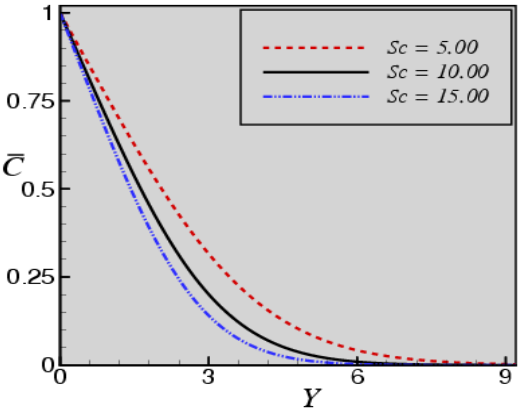

(d)

Figure 8: Concentration profile for Sc at $Pr = 1.00$, $\alpha = 2.00$, $Gr = 6.00$, $Gm = 3.00$ (a) $\tau = 10$ (b) $\tau = 20$ (c) $\tau = 50$ (d) $\tau = 80$.

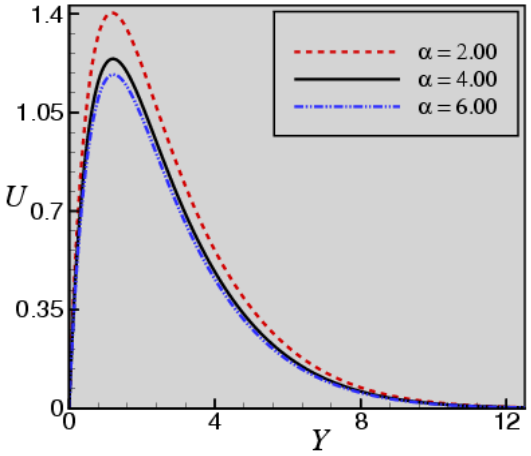

(a)

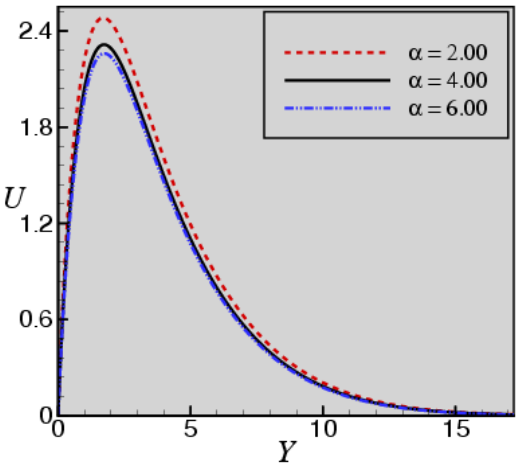

(b)

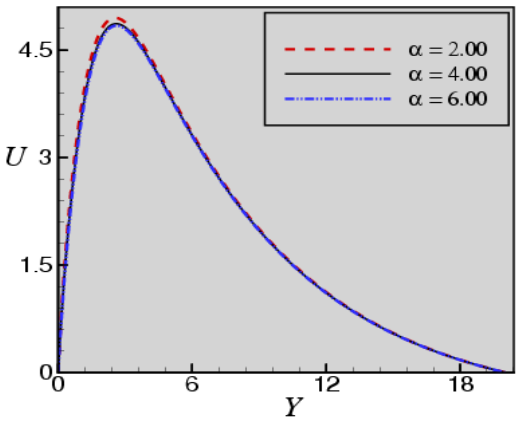

(c)

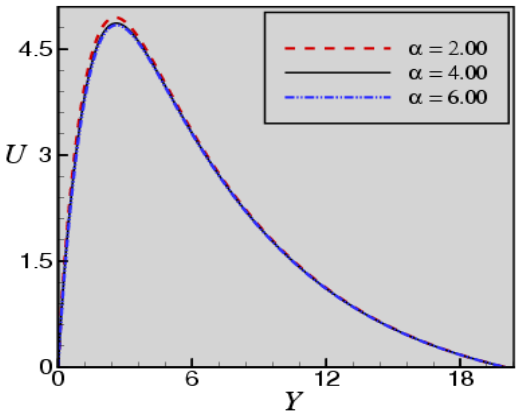

(d)

Figure 9: Velocity profile for α when $Pr = 7.0$, $Gm = 3.00$, $Gr = 6.00$, $Sc = 15.00$ (a) $\tau = 10$, (b) $\tau = 20$, (c) $\tau = 50$ and (d) $\tau = 80$.

Figure 9 represents the velocity profile for different values of the heat source parameter at different time. From Figure 9(a) and Figure 9(b), we found that the velocity profile decreases with the increase of α. but Figure 9(c) and Figure 9(d) show that the velocity profile is steady at α = 4.00, 6.00. Figure 10 represents the temperature profile for different values α at different time. We notice that with the increase of α, the temperature profile decreases at different time. Figure 11 shows the concentration profiles for different values of α at different time. We also notice that temperature profile is steady with the increases of α at different time.

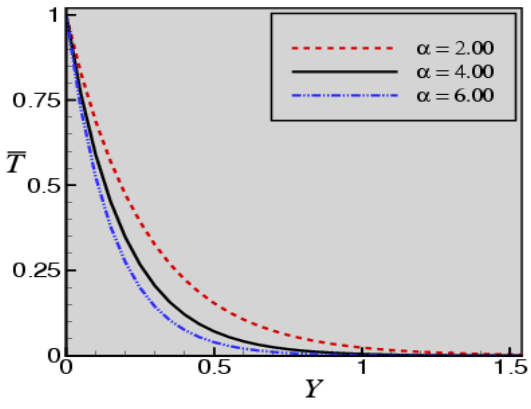

(a)

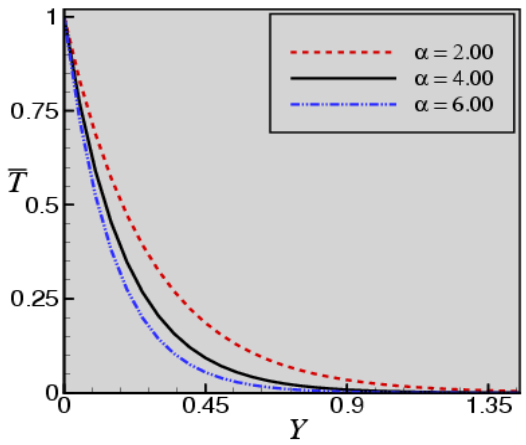

(b)

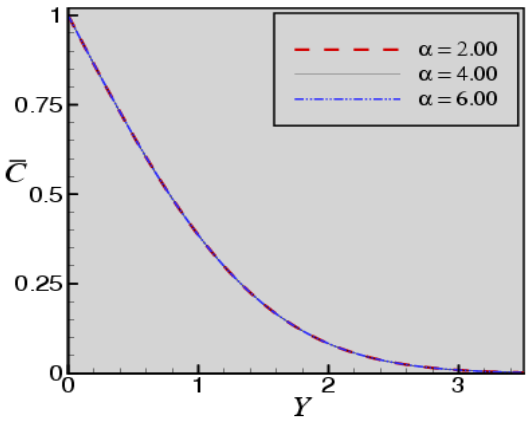

(a)

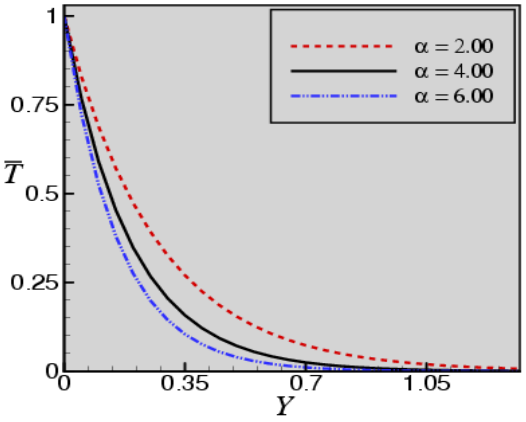

(c)

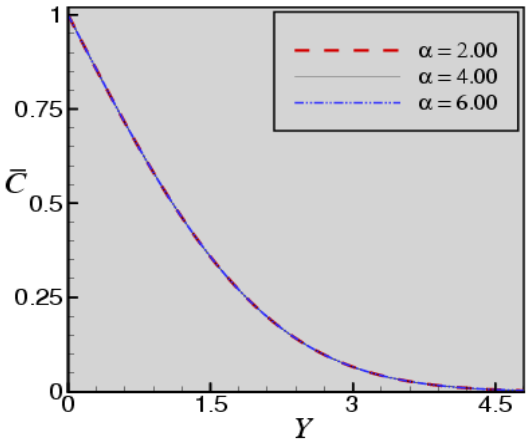

(b)

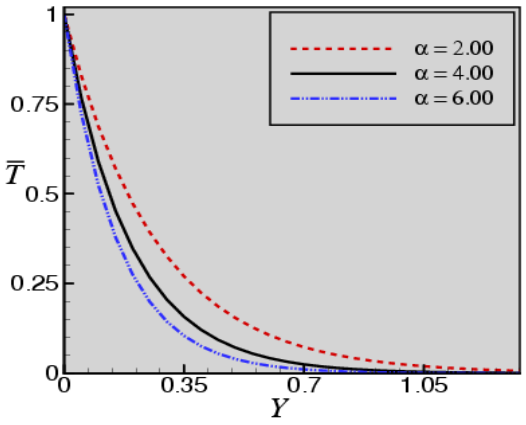

(d)

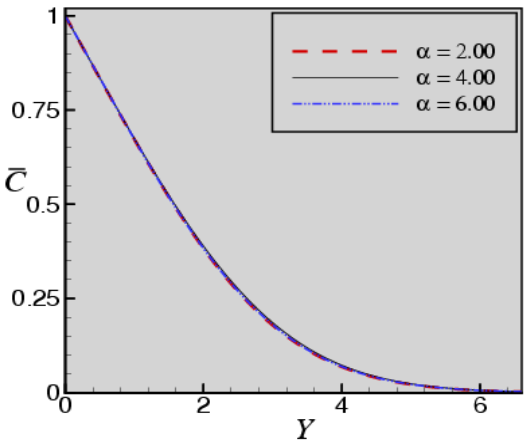

(c)

Figure 10: Temperature profile for α at $Pr = 7.00$, $Gm = 3.00$, $Gr = 6.00$, $Sc = 15.00$ (a) $\tau = 10$ (b) $\tau = 20$ (c) $\tau = 50$ (d) $\tau = 80$.

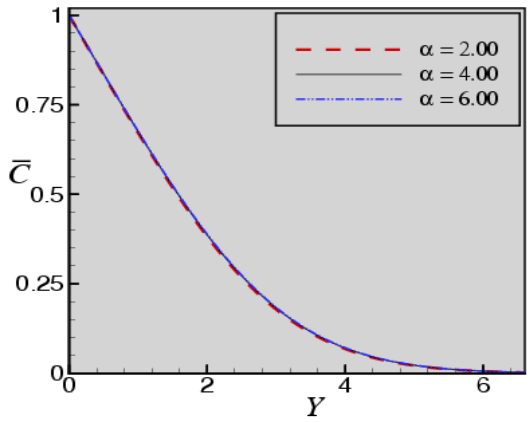

(d)

Figure 11: Concentration profile for α at $Pr = 7.00$, $Gm = 3.00$, $Gr = 6.00$, $Sc = 15.00$ (a) $\tau = 10$ (b) $\tau = 20$ (c) $\tau = 50$ (d) $\tau = 80$.

6. Conclusion

In this paper the thermal boundary layer equations have been derived from Navier-Stokes and concentration equation by boundary layer technique. Some dimensionless variables have been used into Boundary layer equations for providing better understanding of the physical situation. The boundary layer equations are transformed into non-linear partial differential equations by using dimensionless variable. These equations are solved numerically by using finite difference method. Finite difference solution of heat and mass transfer flow is studied to examine the velocity, temperature and concentration distribution characteristics. The effects of different kind of parameters have been examined on the flow with the help of graphs. Different values of Pr, Gr, Gm, Sc and α has been used for obtaining steady-state solutions for the non-dimensional velocity U, temperature $\bar{T}$ and concentration $\bar{C}$ at various dimensionless time τ =10, 20, 50, 80. Along with the steady state solutions, the solutions for the transient values of U versus Y, $\bar{T}$ versus Y and $\bar{C}$ versus Y are obtained. The calculation shows graphical changes in the mentioned quantities up to time τ = 40. Then we notice that at τ = 50-80 the graphical change is negligible. Thereby at dimensionless time τ = 80, the solutions are essentially steady-state solutions.

References

[1] Sparrow, E. M., Eichorn, E and Gregg, J. L., (1959). Combined forced and free convection in boundary layer flow, Phys. of Fluids, Vol. 2, pp. 319-328.

[2] Banthiya, K. K. A. N., (1977). Mixed convection over a semi-infinite vertical flat plate, J. Appl. Math. Phys. Vol. 16, pp. 1958-1963.

[3] Hussain, T. and Afzal, N., (1988). Computer extension of perturbation series for mixed convection on a vertical plate: favourable and adverse flows, Fluid Dynamics Res. Vol. 4, pp. 107-121.

[4] Merkin, J. H., Pop, I and Mohmood, T., (1991). Mixed convection on a vertical surface with a prescribed heat flux; the solution for small and large Prandtl numbers, J. Eng. Math., Vol. 25, pp. 165-190.

[5] Watanabe, T. (1991). Forced and free convection boundary layer flow with uniform suction or injection on a vertical plat plate, Acta Mech., Vol. 89, pp. 123-132.

[6] Cess, R. D., (1966). Int. J. Heat and Mass Trans., Vol. 9, pp.1269

[7] Bestman, A. R., (1990). Int. J. Energy Res., Vol.14, pp. 389.

[8] Mansour, M. A., (1990). Astrophys. Space Sci., Vol. 168, pp. 177.

[9] Alabraba, M. A., Bestman, A. R. and Ogulu, A., (1992). Astrophysics. Space Sc., Vol. 195, pp. 431.

[10] Das, S. S., Tripathy, V. K. and Das, J. K., (2010). Hydrodynamics convective flow past a vertical porous plate through a porous medium with suction and heat source. International Journal of Energy and Environment, Vol. I, pp.467-478.

[11] Sattar, M. A. and Alam, M. M., (1992). Unsteady hydromagnetic free convection flow with hall current and mass transfer along an accelerated porous plate with time dependent temperature and concentration, Canadian J. Phys., Vol. 70, pp. 369.

[12] Alam, M. M., Islam, M. R. and Rahman, F., (2008). Study heat and mass transfer by mixed convection flow from a vertical porous plate with induced magnetic field, constant heat and mass fluxes, Thammasat Int. J. of Science and Technology, Vol. 13(4), pp.1-12.

[13] Alam, M. M. and Sattar, M. A., (1999). J. of Energy, Heat and Mass Transfer, Vol. 21, pp. 9-20.

[14] Alam, M. S., Rahman, M. M. and Samad, M. A., (2006). Numerical study of the combined free-forced convection and mass transfer flow past a vertical porous plate in a porous medium with heat generation and thermal diffusion, Nonlinear Analysis: Modeling and Control, Vol. 11(4), pp. 331-343.

[15] Islam, M. S., Samsuzzoha, M. Shamim Ara and Islam, xN., (2013). Unsteady solutions of thermal boundary layer equations by using finite difference method, Annals of Pure and Applied Mathematics, Vol. 3(2), pp. 142-154.

[16] Chamkha, A. J. and Khaled, A., (2001). Simultaneous heat and mass transfer in free convection, Industrial Engineering Chemical, Vol. 49, pp. 961-968.

[17] Reddy, M.G. and Reddy, N. B., (2011). Journal of Applied Fluid Mechanics, Vol. 4, pp. 27-39.

[18] Hasanuzzaman, M., Mondal, Bichakshan and Touhid Hossain, M. M., (2014). A Study of Similarity Solution of Unsteady Combined Free and Force Convective Laminar Boundary Layer Flow About a Vertical Porous Surface with Suction and Blowing, Annals of Pure and Applied Mathematics, Vol. 6(1), pp. 85-97.